Visual Feedback Sliding-Mode Control of an Overhead Crane System

Li-Jen Shang[1], Kuo-Kai Shyu[2], Chien-Hsing Liao[3]
[1]Associate Professor, Dept. of Computer and Communication Engineering, De-Lin Institute of Technology
[2]Professor, Dept. of Electrical Engineering, National Central University
[3]Lecturer, Dept. of Computer and Communication Engineering, De-Lin Institute of Technology

Abstract

In this study, an anti-swing control scheme and trolley positioning using visual feedback for an underactuated overhead crane system is proposed. It is hard to minimize load swing angle and maximize the speed of load transfer simultaneously by using fewer actuators; moreover, system performance is deteriorated by uncertain parameter and unknown friction. This study proposes a sliding-mode control (SMC) to solve the problems. The sliding surface is designed to couple the trolley dynamics with load-swing dynamics so that the load-swing dynamics is stabilized by injecting the damping effect into the dynamics of the crane system. Furthermore, the designed SMC provides the robustness to complex nonlinear dynamics, unknown load variation and friction. Without using the encoder and/or angle detector mounted on the rotor, this study uses visual signal instead to feedback the system states. A prototype visual feedback crane system is built to verify the proposed algorithm. Experiment results are provided to demonstrate the effectiveness of the proposed visual feedback sliding mode control of the overhead crane system.

Keyword：Visual feedback, Sliding mode, Crane

視覺回授滑動模式控制於天車系統

尚立人[1] 徐國鎧[2] 廖建興[3]

[1]德霖技術學院 電腦與通訊工程系 副教授

[2]國立中央大學 電機工程學系 教授

[3]德霖技術學院 電腦與通訊工程系 助理教授

摘要

本研究提出減少搖擺控制方案，並且使用一個非校正的視覺回授天車系統，改善控制器對天車的操控方式使裝載搖擺角度減到最小和同時具有最快裝載移動的速度，而且系統性能不受不定的參數變量和未知的摩擦力所影響。本研究中我們利用滑動模式控制(SMC)的方法來設計控制器，滑動面被設計結合天車動力學與裝載搖擺動力學，以便裝載移動時產生搖擺經由滑動模式控制可減少裝載搖擺量近而穩定天車系統。 此外，所設計的SMC提供強健控制能力克服裝載變異和摩擦使得天車能在最短的時間內，到達所指定的定點，本文採用視覺回授沒有使用編碼器和角度探測器，主要利用視覺回授信號控制天車的移動。 依據本文所提滑動模式控制法實際建立原型視覺回饋天車系統並提供實驗結果驗證所提的天車系統視覺回授滑動模式控制的效率。

關鍵字：視覺回授、滑動模式、天車

I. INTRODUCTION

Overhead cranes are widely used in industry transportation systems and/or rehabilitation equipments. However, nonlinear dynamics of the overhead crane make the control difficult. Moreover, the crane system is a typical underactuated system, which means that the degree of freedom to be controlled is more than the number of actuators. Therefore it is difficult to control the system dynamics using fewer actuators. Furthermore, the precise transfer of suspend load associated with undesirable load-swing is always deteriorated by the system uncertainties. Accordingly, to achieve the accurate trolley positioning associated with minimum load-swing angle is not an easy work.

Many papers devoted to the design of control scheme of the crane system have been published. Karkoub and Zribi [1] developed an energy-based nonlinear control associated with a linear state feedback controller. Fang *et al.* [2] considered the regulation problem for the crane system and presented energy-based nonlinear coupling controller to improve transient response. But those methods are valid only for small variation of position and swing-angle.

Based on the linearized time-varying crane model, Giua *et al* [3] proposed an observer based controller. Also, Corriga *et al.* [4] presented an implicit gain-scheduling controller for the linear parameter-varying model of cranes. Furthermore, Piazzi and Visioli [5], applying a dynamic inversion procedure, proposed an observer based controller to guarantee a predetermined oscillation. Hamalinen *et al.* [6] presented an optimal path planning to have a smooth transfer of load. Nevertheless, these approaches had not discussed system robustness to uncertainty and disturbance.

To enhance the system robustness, sliding mode control (SMC) is a well known method. Sakawa and Shinclo [7] proposed a second-order sliding-mode control of crane systems. However, it is valid only for small swing angle. A hierarchical sliding-mode control was designed [8], but it did not guarantee the convergence of the subsystem sliding surface. Lee [9] designed a smooth anti-swing motion law to eliminate the load swing angle. Based on the smooth motion trajectory generation [10], Lee [11] presented a sliding mode based proportional–integral–derivative (PID) controller (SMPID), in which the sliding surface couples load-dynamics with trolley motion for stabilizing load-swing dynamics. But the proposed scheme could not guarantee the globally asymptotical stability and the convergence speed of the system dynamics. Studies mentioned above did not consider the friction effect of trolley. However, friction always exists in practical systems.

In 1980, Sanderson and Weiss [12] introduced taxonomy of visual servo systems. A comprehensive survey on visual servoing can be found in [13]. Traditionally, it is usual to feedback the states of the crane system by using encoder mounted on the motor. Because of vision mimicking the human sense of vision and allowing non-contact measurement of the system,

interest about the research of integration of servoing and vision has been increasing. Matsuo [14] presented an anti-swing control of an overhead crane system by applying a PID+Q controller [15] using vision-based measurement; however, the proposed PID control method is not easy to tune the PID gains to obtain the desired performance. The method of tuning control gains particularly is difficult when facing with complex nonlinearities.

Combining the advantage of visual feedback and robustness of SMC, this study proposed a visual feedback SMC design for anti-swing control of crane systems. The main object of this study is to achieve the stabilizing load-swing dynamics and the accurate trolley positioning simultaneously in spite of the friction and uncertain parameter errors caused by unknown variation of load. The key to stabilize the load-swing dynamics is injecting the damping effect into the swing dynamics of the crane system through the design of the sliding surface. Furthermore, the proposed sliding surface which couples the swing dynamics and trolley motion, could determine the desired damping ratio by properly choosing the parameters of sliding surface. The analysis of swing dynamics when constrained to the sliding surface is provided.

The paper is organized as follows: Section II describes the system including: *A) dynamical model of an overhead crane* and *B) visual measurement and tracking method.* In section III, one has the design of anti-swing control, which consists of *A) stability of the load-swing dynamics* and *B) sliding-mode controller design*. Experimental results are provided, in section IV, to verify the proposed method. Finally, conclusions are drawn in section V.

II. System Description

The visual feedback crane system can be described by two main parts: A). Dynamical model of an overhead crane and B). Visual measurement and tracking method.

A. Dynamical model of an overhead crane

Figure 1 shows an overhead crane system with a suspended load, where x is the trolley displacement, L is the length of the suspension rope, θ denotes the load swing angle. The trolley is driven by a force u, and the load is suspended from the trolley by a rigid rope. In this study, the motion of load is always on the $X-Z$ plane.

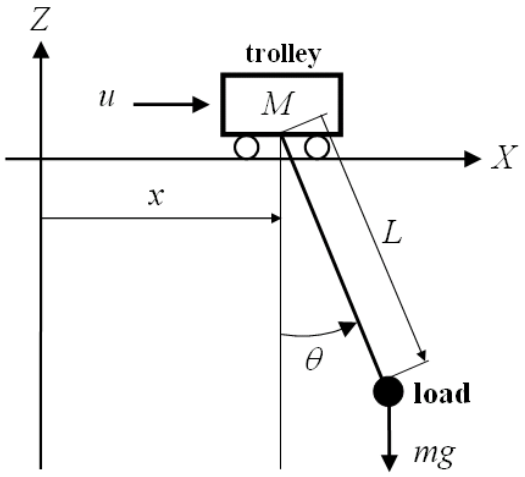

Fig.1. Model of a two-dimensional overhead crane.

The dynamical equations of an overhead crane system subjected to friction can be described as

$$(M+m)\ddot{x} + mL(\ddot{\theta}\cos\theta - \dot{\theta}^2\sin\theta) = u - d(\dot{x},u) \tag{1}$$

$$L\ddot{\theta} + \ddot{x}\cos\theta + g\sin\theta = 0 \tag{2}$$

Where M is the trolley mass, m is the load mass, g denotes the gravitational acceleration, and $d(\dot{x},u)$ is the friction given by (3) and shown in Fig. 2 [16].

$$d(\dot{x},u) = \mu_d(\dot{x})\lambda(\dot{x}) + \mu_s(\dot{x},u)[1-\lambda(\dot{x})] \tag{3}$$

where $\lambda(\cdot)$ is the switching function defined by

$$\lambda(\dot{x}) = \begin{cases} 1 & , |\dot{x}| > \varepsilon \\ 0 & , |\dot{x}| \le \varepsilon \end{cases} \tag{4}$$

with a given constant ε>0, $\mu_d(\dot{x})$ represents the dynamic friction force at nonzero velocity and $\mu_s(\dot{x},u)$ denotes the static friction force at zero velocity.

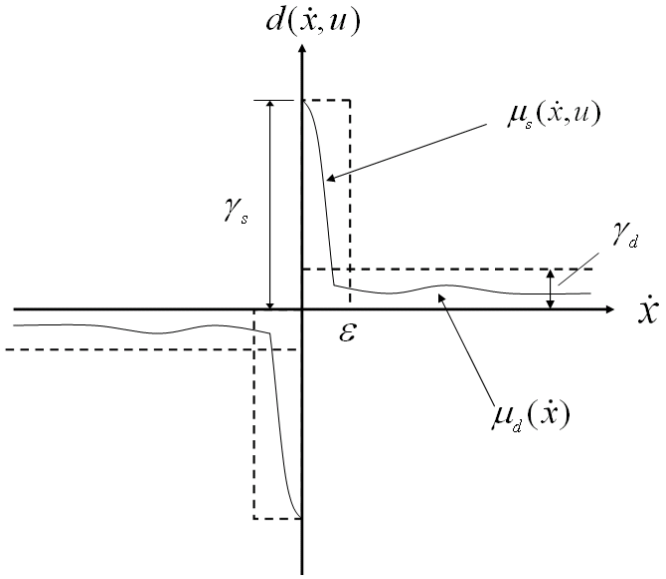

Fig. 2. Unknown friction model

The trolley dynamics (1) with the load-swing dynamics (2) can be rewritten as

$$\ddot{x} = \frac{m(L\dot{\theta}^2 \sin\theta + g\sin\theta\cos\theta)}{M + m\sin^2\theta} + \frac{1}{M + m\sin^2\theta}(u - d(\dot{x},u)) \tag{5}$$

Define the state vector as

$$\underline{q} = [x \quad \dot{x} \quad \theta \quad \dot{\theta}]^T \tag{6}$$

When considering the load mass variation Δm, one has $m = \tilde{m} + \Delta m$, where $\tilde{m}$ is the nominal mass. Then the dynamics equation (5) becomes

$$\begin{aligned} \ddot{x} &= \frac{(\tilde{m} + \Delta m)(L\dot{\theta}^2 \sin\theta + g\sin\theta\cos\theta)}{M + (\tilde{m} + \Delta m)\sin^2\theta} + \frac{1}{M + (\tilde{m} + \Delta m)\sin^2\theta}(u - d(\dot{x},u)) \\ &= f(\underline{q}) + b(\underline{q})(u - d(\dot{x},u)) \\ &= (\tilde{f}(\underline{q}) + \Delta f(\underline{q})) + (\tilde{b}(\underline{q}) + \Delta b(\underline{q}))(u - d(\dot{x},u)) \end{aligned} \tag{7}$$

where $\tilde{f}(\underline{q})$, and $\tilde{b}(\underline{q})$ are the nominal parts of trolley motion dynamics, $\Delta f(\underline{q})$, and $\Delta b(\underline{q})$ are the uncertain parts affected by the load mass variation. The nominal parts of dynamical equations (7) can be represented as

$$\tilde{f}(\underline{q}) = \frac{\tilde{m}(L\dot{\theta}^2 \sin\theta + g\sin\theta\cos\theta)}{M + \tilde{m}\sin^2\theta} \tag{8}$$

$$\tilde{b}(\underline{q}) = \frac{1}{M + \tilde{m}\sin^2\theta} \tag{9}$$

Thus the uncertain parts of (7) can be obtained as

$$\Delta f(\underline{q}) = f(\underline{q}) - \tilde{f}(\underline{q}) \tag{10}$$

$$\Delta b(\underline{q}) = b(\underline{q}) - \tilde{b}(\underline{q}) \tag{11}$$

The aim now is to design a control u such that the trolley position moves along the pre-specified reference input trajectory. Moreover, it has to simultaneously achieve the anti-swing control of load-swing dynamics under the influence of uncertainties and friction.

Before proceeding the design, the following assumptions are made:

Assumption 1: Suppose that the upper bound of the uncertain input matrix is bounded by $\left|\Delta b(\underline{q})\right| < \left|\tilde{b}(\underline{q})\right|$.

Assumption 2: Suppose that $\mu_d(\dot{x})$ and $\mu_s(\dot{x},u)$ are known and uniformly bounded by γ_d and γ_s, respectively. Thus,

$$\left|\mu_d(\dot{x})\right| \le \gamma_d \ , \ \forall\dot{x} \tag{12}$$

$$\left|\mu_s(\dot{x},u)\right| \le \gamma_s \ , \ \forall\dot{x} \ , \ \forall u \tag{13}$$

Assumption 3: The reference input trajectories r_x, $\dot{r}_x$ and $\ddot{r}_x$ are assumed to be uniformly bounded and $\dddot{r}_x$ must be designed to be zero in finite time. On the other hand, the reference trajectory γ_θ of load-swing dynamics is set to be zero in entire control.

Assumption 4: Suppose that the initial swing angle $\left|\theta(0)\right| < \pi/2$ and the suspension rope length satisfies $0 < L < L_{\max}$.

B. Visual measurement and tracking method

The visual sensor consists of a CCD camera and an image grabber. The image is taken with rate of 30 pictures per second. Two markers are made on the trolley and load respectively for tracking so that the trolley position and load swing angle can be measured. The system configuration of the visual servo crane system is depicted in Fig. 3.

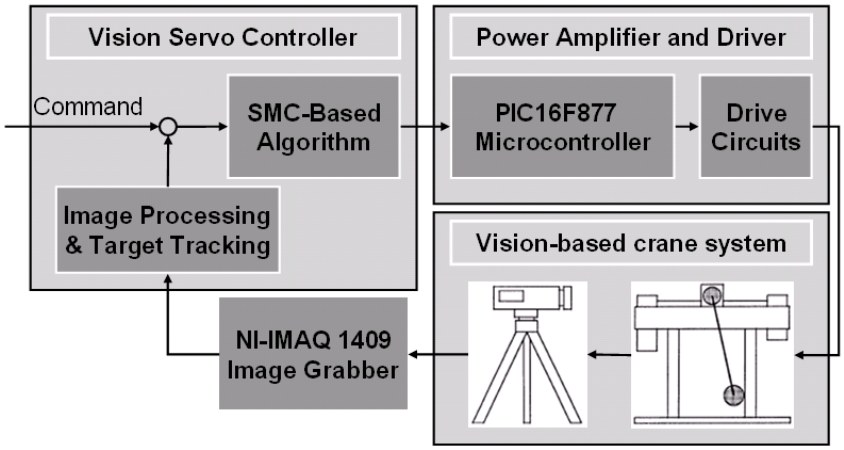

Fig.3. System configuration of the visual feedback crane system.

It is straightforward to search the target from an image. The target tracking from the image information is accomplished by the template matching using cross-correlation algorithm. Generally, the target of interest is chosen as the template in advance. Then, the most similar block with respect to the template is located as the target position on the image. The similarity between the template of the target and the most similar area of the current image is determined by the following formulation

$$\varphi_{ts} = \frac{\vec{t} \cdot \vec{s}}{\|\vec{t}\|\|\vec{s}\|} \tag{14}$$

where $\varphi_{ts} \in [0,1]$ is a positive constant equivalent to the similarity between $\vec{t}$ and $\vec{s}$, respectively. Where $\vec{t}$ and $\vec{s}$ are grey value vectors of the template and the possibly similar area of the current image. The new target position is obtained when the maximum of φ_{ts} is found in current image. The control command is thus computed according to the error between the new position and the desired one. Then the control command is transferred to the motor driver of crane by RS232C at the rate of 19200 bits/second.

III. Design of Anti-swing Control

An anti-swing control will be designed based on the sliding-mode control in this section. It will be designed so that the trolley dynamics and load-swing dynamics is coupled on the sliding surface. Moreover, a sliding-mode controller is given to guarantee the whole system stability despite the system uncertainties and friction.

First, define the tracking error $e(t)$ corresponding to the reference input trajectory

$$e(t) = \begin{bmatrix} e_x \\ e_\theta \end{bmatrix} = \begin{bmatrix} r_x - x \\ r_\theta - \theta \end{bmatrix} = \begin{bmatrix} r_x - x \\ -\theta \end{bmatrix} \tag{15}$$

where r_x and $r_\theta = 0$ are the reference trajectories of trolley position and load-swing respectively.

Next, define the sliding surface s which couples the trolley motion and swing dynamics, be

$$s = \dot{e}_x + ce_x - k_\theta e_\theta = \dot{e}_x + ce_x + k_\theta \theta \tag{16}$$

where c, and k_θ are positive constants. Once the system dynamics of the crane are restricted on the sliding surface $s = 0$, the stability of entire system is equivalent to the stability of the sliding surface that depends on the trolley position tracking error.

A. Stability of the load-swing dynamics

Suppose that s is controlled to be zero for all time $t \geq t_s > 0$. Then, (16) is rewritten as

$$\dot{e}_x + ce_x = -k_\theta \theta \tag{17}$$

Therefore, one has

$$e_x(t) = e_x(t_s)e^{-c(t-t_s)} - k_\theta \int_{t_s}^{t} \theta(\tau)e^{c(\tau-t)}d\tau \tag{18}$$

On the sliding surface $s = 0$, $\ddot{x}$ has the form as $\ddot{x} = \ddot{r}_x + c\dot{e}_x + k_\theta \dot{\theta}$. Then one sees that $\ddot{x}$ can be viewed as an input to the load-swing dynamics (2). As a consequence, (2) can be rewritten as

$$\begin{aligned} &L\ddot{\theta} + k_\theta \cos\theta\dot{\theta} + g\sin\theta - ck_\theta \cos\theta(\theta - \phi(\theta)) \\ &= (c^2 e_x(t_s)e^{-c(t-t_s)} - \ddot{r}_x)\cos\theta \end{aligned} \tag{19}$$

where

$$\phi(\theta) = \int_{t_s}^{t} \theta(\tau)e^{c(\tau-t)}d\tau \tag{20}$$

Note that the magnitude of $\phi(\theta)$ is smaller than or equal to that of θ/c [11]. As a consequence, $\left|ck_\theta \cos\theta(\theta - \phi(\theta))\right|$ is much smaller in magnitude than $g\sin\theta$ if $ck_\theta << g$. Then $ck_\theta \cos\theta(\theta - \phi(\theta))$ can be neglected safely relative to $g\sin\theta$. Therefore, the kinematical equation (19) can be reduced to the following form

$$L\ddot{\theta} + k_\theta \cos\theta\dot{\theta} + g\sin\theta = (c^2 e_x(t_s)e^{-c(t-t_s)} - \ddot{r}_x)\cos\theta \tag{21}$$

The sliding surface parameter k_θ is designed to guarantee the asymptotic vanishing of the load-swing dynamics (21).

Theorem 1: The load-swing dynamics of (21) is asymptotically stable, if $k_\theta > 0$ and there is a positive constant ψ satisfying $k_\theta \cos\theta \geq \psi$.

Proof: Consider the following Lyapunov function candidate：

$$V_\theta = \frac{1}{2} L\dot{\theta}^2 + g(1-\cos\theta) \tag{22}$$

Taking the time derivative of V_θ yields

$$\begin{aligned} \dot{V}_\theta &= L\dot{\theta}\ddot{\theta} + g\dot{\theta}\sin\theta \\ &= -k_\theta\dot{\theta}^2\cos\theta + (c^2 e_x(t_s)e^{-c(t-t_s)} - \dddot{r}_x)\dot{\theta}\cos\theta \end{aligned} \tag{23}$$

There exists a constant ψ such that $k_\theta \cos\theta \geq \psi$, (23) can be reduced as

$$\dot{V}_\theta(t) \leq -\psi\dot{\theta}^2 + (c^2|e_x(t_s)|e^{-c(t-t_s)} - |\dddot{r}_x|)|\dot{\theta}| \tag{24}$$

Because $\dddot{r}_x$ is designed to be zero for all time $t \geq t_f$, where t_f is a finite positive constant, $\dot{V}_\theta \leq 0$ is guaranteed for all $\psi|\dot{\theta}| \geq (c^2 e_x(t_s)e^{-c(t-t_s)} - \dddot{r}_x)$. Hence $\theta(t) \in L_\infty$ and $\dot{\theta} \in L_\infty$. Integrating (24) yields

$$0 \leq V_\theta(t) \leq V(0) - \int_0^t \psi\dot{\theta}^2 d\tau + \int_0^t (c^2|e_x(t_s)|e^{-c(t-t_s)} - |\dddot{r}_x|)|\dot{\theta}|d\tau \tag{25}$$

Rearranging (25) and letting time approaches infinite, one obtains

$$\lim_{t\to\infty}\int_0^t \psi\dot{\theta}^2 d\tau \leq V(0) + \lim_{t\to\infty}\int_0^t (c^2|e_x(t_s)|e^{-c(t-t_s)} - |\dddot{r}_x|)|\dot{\theta}|d\tau \tag{26}$$

Note that the last term on the right side of (26) is bounded. According to *Barbalet's Lemma* [17], one has $\dot{\theta} \to 0$ asymptotically as $t \to \infty$, which also guarantees $\ddot{\theta} \to 0$ asymptotically as $t \to \infty$. Then kinematical equation (21) guarantees $\theta \to 0$ asymptotically as $t \to \infty$. And it also implies that the $e_\theta, \dot{e}_\theta, \ddot{e}_\theta \to 0$ asymptotically as $t \to \infty$ since $r_\theta = 0$ throughout the entire control. Thus, equation (21) guarantees $x \to r_x$ asymptotically as $t \to \infty$.

Q.E.D.

B. Sliding-mode controller design

An anti-swing control for crane system described by (1) and (2) will be proposed in the following theorem.

Theorem 2: Consider an overhead crane system whose dynamics is described by the trolley dynamics (1) and load-swing dynamics (2). The sliding surface s, (16), is asymptotically stable in finite time, if the following control (27) is given

$$u = \frac{1}{\tilde{b}(q) - \beta}(\tilde{u} + (\alpha + \eta|\tilde{u}|)\mathrm{sgn}(s)) + k_f(\dot{x}, s) + ks \tag{27}$$

with

$$\tilde{u} = \ddot{r}_x + c\dot{e}_x(t) + k_\theta \dot{\theta} - \tilde{f}(\underline{q}) \tag{28}$$

and

$$k_f(\dot{x}, s) = \begin{cases} \gamma_s \,\mathrm{sgn}(s), & |\dot{x}| \le \varepsilon \\ \gamma_d \,\mathrm{sgn}(s), & |\dot{x}| > \varepsilon \end{cases} \tag{29}$$

where k is a positive constant and $\eta > 1$.

***Proof*：** The Lyapunov function is firstly defined as:

$$V = \frac{1}{2}s^2 \tag{30}$$

Differentiating $V(t)$ with respect to time t obtains：

$$\begin{aligned} \dot{V} &= s\dot{s} \\ &= s(\tilde{u} - \Delta f(\underline{q}) - b(\underline{q})u + b(\underline{q})g(\dot{x}, u)) \end{aligned} \tag{31}$$

Inserting u into above equation, one obtain

$$\begin{aligned} \dot{V} &= s\left[\tilde{u} - \Delta f(\underline{q}) - b(\underline{q})\left(\frac{\tilde{u} + (\alpha + \eta|\tilde{u}|)\mathrm{sgn}(s)}{\tilde{b}(\underline{q}) - \beta} - k_f(\dot{x}, s) - ks\right)\right] + b(\underline{q})g(\dot{x}, u)s \\ &\le |\tilde{u}||s| + |\Delta f(\underline{q})||s| - \frac{b(\underline{q})}{\tilde{b}(\underline{q}) - \beta}(\alpha + (\eta + 1)|\tilde{u}|)|s| - \gamma_s b(\underline{q})|s| + g(\dot{x}, u)b(\underline{q})|s| - b(\underline{q})ks^2 \\ &\le -\left(\frac{\eta\tilde{b}(\underline{q}) + \eta\Delta b(\underline{q})) + \beta + \Delta b(\underline{q})}{\tilde{b}(\underline{q}) - \beta}\right)|\tilde{u}||s| - b(\underline{q})ks^2 \\ &\le -\sigma s^2 \end{aligned} \tag{32}$$

where $\sigma = \min(kb(\underline{q}))$, k, and σ are nonzero positive constants. The term $b(\underline{q})$ is always positive and uniformly bounded described in (7).Therefore (32) ensures that sliding surface is asymptotically stable which means $s \to 0$ in finite time.

Q.E.D.

IV. Experiment Results

Experimental results are provided to verify the effectiveness of the proposed SMC based anti-swing control using visual feedback, in the section. The experimental system is shown in Figure 4. System parameters are given as: M =3kg, m =1.6kg, L =0.6m, and the max speed of trolley 0.34 m/sec. The sliding surface parameters are given as: c =0.969 and k_θ =0.101. The

system sampling rate 30Hz is limited by the capacity of camera and the image grabber. Besides, the camera is set to 0.5 m in front of the crane. The relation between pixels on the feedback image and actual moving distance is about 525 pixel/m.

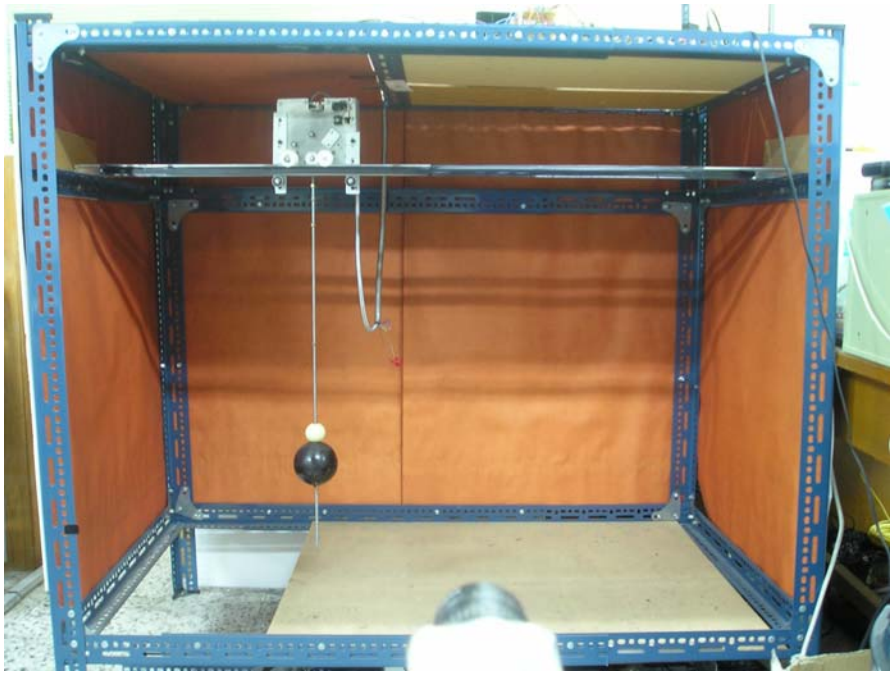

Fig. 4. Visual feedback overhead crane system.

A similar control method using SMPID[15], which has the same slide surface but does not assure the sliding motion, is used for comparison with the presented SMC method using visual feedback.

The experiments, for both SMPID and SMC using visual feedback, of positioning 0.8meter within 5sec without disturbance are firstly tested and shown in Fig. 5. Figs. 5(a) and 5(b) respectively show the trolley position response and load swing angle response controlled by SMPID [11] and the proposed SMC. Figure 5(c) and 5(d) are the related error responses in image in pixels of 5(a) and 5(b) respectively. Observing Figs. 5(a)-(d), one sees that there is overshoot trolley position response of SMPID but not of SMC. And both SMPID and SMC have similar swing angle responses.

Next, to verify the robustness to external disturbance of the system controlled by both methods, an impulse disturbance is added to move the load away from its steady state position. The impact disturbance is added to the load at time about t =12 sec. Dynamic responses as Figures 5(a)-(d) are also shown in Figures 6(a)-(d) respectively. It can be seen from Fig. 6 that the proposed control method provides better robustness than [15].

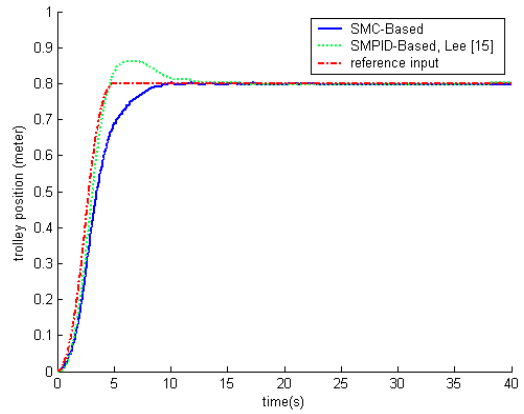

(a) Trolley position

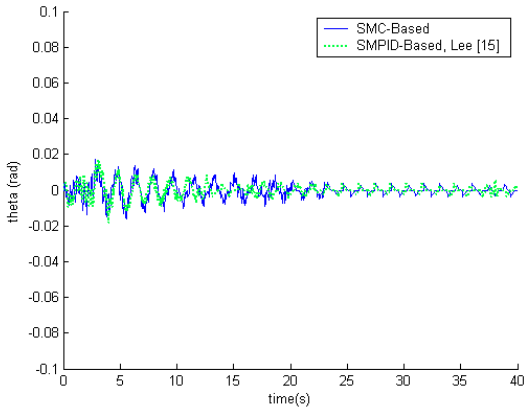

(b) Load swing angle

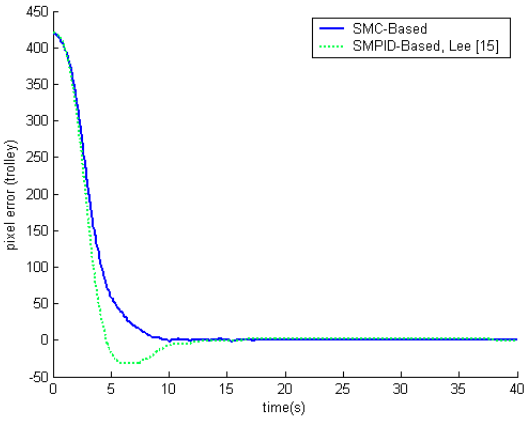

(c) Pixel errors of trolley position

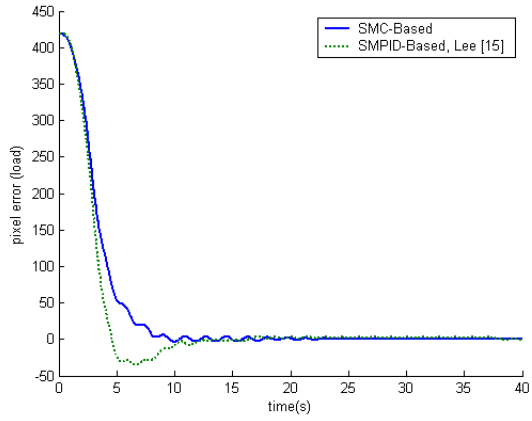

(d) Pixel errors of load swing angle

Fig. 5. Experiment (without disturbance): SMC and SMPID based methods ($k_p = 100, k_I = 80$).

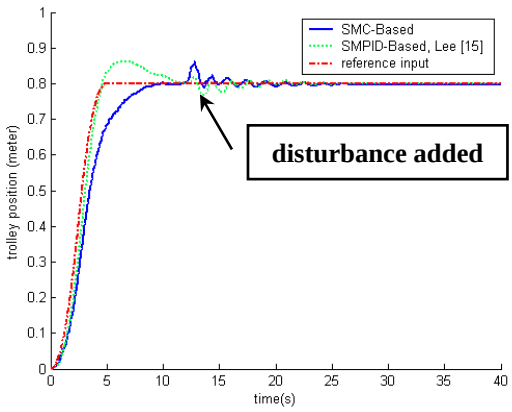

(a) Trolley position

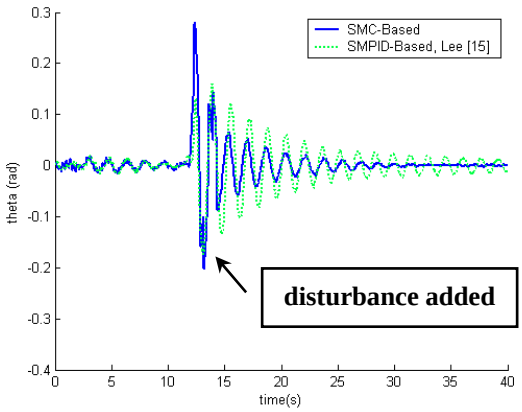

(b) Load swing angle

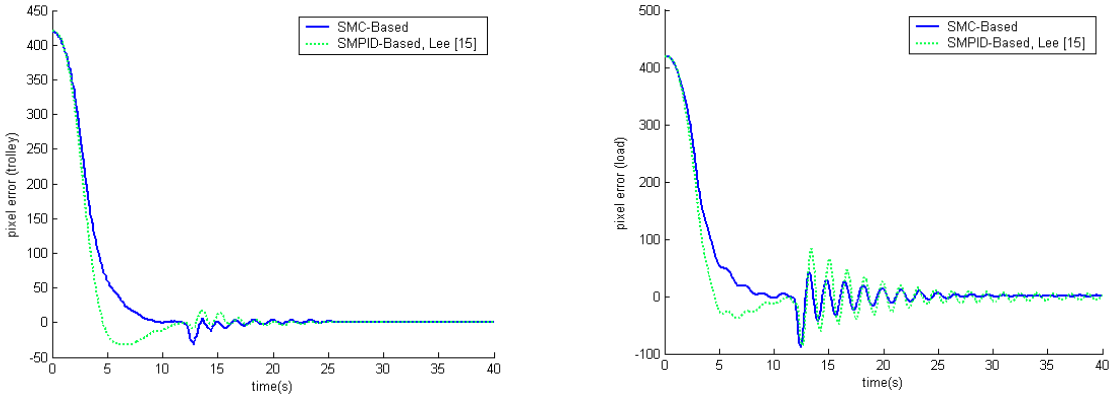

(c) Pixel errors of trolley position (d) Pixel errors of load swing angle

Fig. 6. Experiment (with disturbance): SMC and SMPID based methods ($k_p = 100, k_I = 80$).

V. Conclusions

The problem of transporting an uncertain suspended load has been addressed. Without using encoder mounted on the rotor of the trolley to feedback system states, this paper uses image instead as the feedback signal. The proposed visual feedback control achieves anti-swing control based on sliding motion. The sliding surface is designed to couple the load-swing dynamics with trolley motion dynamics. Thus one allows the direct design of damping ratio and guarantees the stability of swing dynamics; on the other hand, trolley motion still tracks the reference trajectory in spite of uncertainties. Moreover, a prototype visual crane system has been built to demonstrate the effectiveness of the control method. Experimental results verify that the proposed control guarantees the stability of anti-swing dynamics when subjected to external disturbance.

VI. References

[1] M.A. Karkoub and M. Zribi, "Modelling and energy based nonlinear control of crane lifters," *IEE Proc.-Control Theory Application*, vol. 149, no. 3, pp. 209-216, 2002.

[2] Y. Fang, W. E. Dixon, D.M. Dawson and E. Zergeroglu, "Nonlinear coupling control laws for an underactuated overhead crane system," *IEEE/ASME Transaction on Mechatron*, vol.8, no. 3, pp. 418-423, 2003.

[3] A. Giua, C. Seatzu and G. Usai, "Observer-controller design for cranes via Lyapunov equivalence," *Automatica*, vol. 35, no. 4, pp. 669-678, 1999.

[4] G. Corriga, A. Giua and G. Usai, "An implicit gain-scheduling controller for cranes," *IEEE Trans. Contr. Syst.*, vol. 6, no. 1, pp. 15-20, 1998.

[5] A. Piazzi and A. Visioli, "Optimal dynamic inversion based control of an overhead crane," *IEE Proc-Control Theory Application*, vol. 149, no. 5, pp. 405-411, 2002.

[6] J.J. Hamalinen, A. Marttinen, L. Baharova and J. Virkkunen, “Optimal path planning for a trolley crane fast and smooth transfer of load,” *IEE Proc.-Control Theory Application*, vol. 142, no. 1, pp. 51-57, 1995.

[7] Sakawa and Y. Shindo, “Optimal control of container cranes,” *Automatica*, vol. 18, no. 3, pp. 257-266, 1982.

[8] W. Wang, J. Yi, D. Zhao and D. Liu, “Design of a stable sliding-mode controller for a class of second-order underactuated systems,” *IEE Proc. -Control Theory App.* , vol. 151, no. 6, pp. 683-690, 2004.

[9] H. H. Lee, “Motion planning for three-dimensional overhead cranes with high-speed load hoisting,” *Int. J. Control*, vol. 78, no. 12, pp. 875-886, 2005.

[10] H.-H. Lee, “A new motion-planning scheme for overhead cranes with high-speed hoisting,” *ASME Transactions, Journal of Dynamic Systems, Measurement, and Control*, vol. 126, pp. 359–364, 2004.

[11] H. H. Lee, “A new design approach for the anti-swing trajectory control of overhead cranes with high-speed hosting,” *Int. J. Control*, vol. 77, no. 10, pp. 931-940, 2004.

[12] A. C. Sanderson, and L. E. Weiss, “Image-based visual servo control using relational graph error signals,” *Proceedings of the IEEE International Conference on Robotics and Automation*, pp. 1074-1077, 1980.

[13] S. Hutchinson, G. Hager and P. Corke, “A tutorial on visual servo control,” *IEEE Trans. Robotics Automat*., vol. 12, no.5, pp. 651–670, Oct. 1996.

[14] T. Matsuo, R. Yoshino, H. Suemitsu, and K. Nakano, “Nominal performance recovery by PID+Q controller and its application to antisway control of crane lifter with visual feedback,” *IEEE Tran. Contr. Sys. Tech.*, vol. 12, no. 1, pp.156-166, 2004.

[15] T. Matsuo and K. Nakano, “Robust stabilization of closed-loop systems by PID+Q controller,” *Int. J. Control*, vol. 70, no. 4, pp. 631-650, 1998.

[16] C. T. Johnson and R. D. Lorenz, “Experimental identification of friction and its compensation in precise, position controlled mechanisms,” *IEEE Trans. Industry Application*, vol. 28, no. 6, pp. 1392-1398, 1992.

[17] H. K. Khalil, *Nonlinear systems*, 3rd Edition, Prentice Hall, 2002.